1   **Greenhouse gas fluxes in mangrove forest soil in an Amazon estuary**

2   Saúl Edgardo Martínez Castellón[1], José Henrique Cattanio[1*], José Francisco Berrêdo[1;3],
3   Marcelo Rollnic[2], Maria de Lourdes Ruivo[1;3], Carlos Noriega[2].
4   [1] Graduate Program in Environmental Sciences. Federal University of Pará, Belém,
5   Brazil
6   [2] Marine Environmental Monitoring Research Laboratory. Federal University of Pará,
7   Belém, Brazil.
8   [3] Department of Earth Sciences and Ecology. Paraense Emílio Goeldi Museum, Belém,
9   Brazil
10   [*] Corresponding author: cattanio@ufpa.br (J.H. Cattanio)

11   Abstract: Tropical mangrove forests are important carbon sinks, the soil being the main

12   carbon reservoir. Understanding the variability and the key factors that control fluxes is

13   critical to accounting for greenhouse gas (GHG) emissions, particularly in the current

14   scenario of global climate change. This study is the first to quantify methane (CH_4) and

15   carbon dioxide (CO_2) emissions using a dynamic chamber in a natural mangrove soil of

16   the Amazon. The plots for the trace gases study were allocated at contrasting

17   topographic heights. The results showed that the mangrove soil of the Amazon estuary

18   is a source of CO_2 (6.66 g CO_2 m^{-2} d^{-1}) and CH_4 (0.13 g CH_4 m^{-2} d^{-1}) to the atmosphere.

19   The CO_2 flux was higher in the high topography (7.858 g CO_2 m^{-2} d^{-1}) than in the low

20   topography (4.734 g CO_2 m^{-2} d^{-1}) in the rainy season, and CH_4 was higher in the low

21   topography (0.128 g CH_4 m^{-2} d^{-1}) than in the high topography (0.014 g CH_4 m^{-2} d^{-1}) in

22   the dry season. However, in the dry period, the low topography soil produced more

23   CH_4. Soil organic matter, carbon and nitrogen ratio (C/N), and redox potential

24   influenced the annual and seasonal variation of CO_2 emissions; however, they did not

25   affect CH_4 flux. The mangrove soil of the Amazon estuary produced 35.4 Mg CO_{2-eq} ha^{-1} y^{-1}. A total of 2.16 kg CO_2 m^{-2} y^{-1} needs to be sequestered by the mangrove ecosystem

27   to counterbalance CH_4 emissions.

28   **1   Introduction**

29   The mangrove areas are estimated to be the main contributors to greenhouse gas

30   emissions in marine ecosystems (Allen et al., 2011; Chen et al., 2012). However,

31   mangrove forests are highly productive due to a high nutrient turnover rate (Robertson

32   et al., 1992) and have mechanisms that maximize carbon gain and minimize water loss

33   through plant transpiration (Alongi and Mukhopadhyay, 2015). A study conducted in 25

34   mangrove forests (between 30° latitude and 73° longitude) revealed that these forests

35 are the richest in carbon storage in the tropics, containing on average 1,023 Mg C ha^{-1} of

36 which 49 to 98% is present in the soil (Donato et al., 2011).

37 The estimated soil CO_2 outgassing, in tropical estuarine areas is 16.2 Tg C y^{-1} (Alongi,

38 2009). However, soil efflux measurements from tropical mangroves revealed emissions

39 ranging from 2.9 to 11.0 g CO_2 m^{-2} d^{-1} (Castillo et al., 2017; Chen et al., 2014; Shiau

40 and Chiu, 2020). In situ CO_2 production is related to the water input of terrestrial,

41 riparian, and groundwater brought by rainfall (Rosentreter et al., 2018b). Due to the

42 periodic tidal movement, the mangrove ecosystem is daily flooded, leaving the soil

43 anoxic and consequently reduced, favoring methanogenesis (Dutta et al., 2013). Thus,

44 estuaries are considered hotspots for CH_4 production and emission (Bastviken et al.,

45 2011; Borges et al., 2015). The organic material decomposition by methanogenic

46 bacteria in anoxic environments, such as sediments, inner suspended particles,

47 zooplankton gut (Reeburgh, 2007; Valentine, 2011), and the impact of freshwater

48 should change the electron flow from sulfate-reducing bacteria to methanogenesis

49 (Purvaja et al., 2004), which also results in CH_4 formation. On the other hand, an

50 ecosystem with salinity levels above 18 ppt may show an absence of CH_4 emissions

51 (Poffenbarger et al., 2011), since methane dissolved in pores is typically oxidized

52 anaerobically by sulfate (Chuang et al., 2016). Currently the uncertainty in emitted CH_4

53 values in vegetated coastal wetlands is approximately 30% (EPA, 2017). Soil flux

54 measurements from tropical mangroves revealed emissions ranging from 0.3 to 4.4 mg

55 CH_4 m^{-2} d^{-1} (Castillo et al., 2017; Chen et al., 2014; Kreuzwieser et al., 2003).

56 The production of greenhouse gases from soils is mainly driven by biogeochemical

57 processes. Microbial activities and gas production are related to soil properties,

58 including total carbon and nitrogen concentrations, moisture, porosity, salinity, and

59 redox potential (Bouillon et al., 2008; Chen et al., 2012). Due to the dynamics of tidal

60 movements, mangrove soils may become saturated and present a reduced oxygen

61 availability, or suffer total aeration caused by the ebb tide. Studies attribute soil carbon

62 flux responses to moisture perturbations because of seasonality and flooding events

63 (Banerjee et al., 2016), with fluxes being dependent on tidal extremes (high tide and low

64 tide), and flood duration (Chowdhury et al., 2018). In addition, phenolic compounds

65 inhibit microbial activity and help keep organic carbon intact, thus leading to the

66 accumulation of organic matter in mangrove forest soils (Friesen et al., 2018).

67 The Amazonian coastal areas in the State of Pará (Brazil) cover 2,176.8 km^2 where

68 mangroves develop under the macro-tide regime (Souza Filho, 2005), representing

69 approximately 85% of the entire area of Brazilian mangroves (Herz, 1991). The

70 objective of this study is to investigate the monthly flux of CO_2 and CH_4 from the soil,

71 at two topographic heights, in a pristine mangrove area in the Mojuim River Estuary,

72 belonging to the Amazon biome. The gas fluxes were studied together with the analysis

73 of the vegetation structure and soil physical-chemical parameters.

74 **2   Material and Methods**

75 **2.1   Study site**

76 This study was conducted in the Amazonian coastal zone, Macaca Island (-0.746491

77 latitude and -47.997219 longitude), located in the Mojuim River estuary, at the

78 Mocapajuba Marine Extractive Reserve, municipality of São Caetano de Odivelas

79 (Figure 1), state of Pará (Brazil). The Macaca island has an area of 1,322 ha of pristine

80 mangroves, which belongs to a mangrove area of 2,177 km^2 in the state of Pará (Souza

81 Filho, 2005). The climate is type Am (tropical monsoon) according to the Köppen

82 classification (Peel et al., 2007). The climatological data were obtained from the

83 Meteorological Database for Teaching and Research of the National Institute of

84 Meteorology (INMET). The area has a rainy season from January to June (2,296 mm of

85 precipitation) and a dry season from July to December (687 mm). March and April were

86 the rainiest months with 505 and 453 mm of precipitation, while October and November

87 were the driest (53 and 61 mm, respectively). The minimum temperatures occur in the

88 rainy period (26 °C) and the maximum in the dry period (29 °C). The Mojuim estuary

89 has a macrotidal regime, with an average amplitude of 4.9 m during spring tide and 3.2

90 m during low tide (Rollnic et al., 2018). During the wet season the Mojuim River has a

91 flow velocity of 1.8 m s^{-1} at the ebb tide and 1.3 m s^{-1} at the flood tide. During the dry

92 season, the maximum currents reach 1.9 m s^{-1} at the flood and 1.67 m s^{-1} at the ebb tide

93 (Rocha, 2015). The annual mean salinity is 26.95 PSU (Valentim et al., 2018).

94
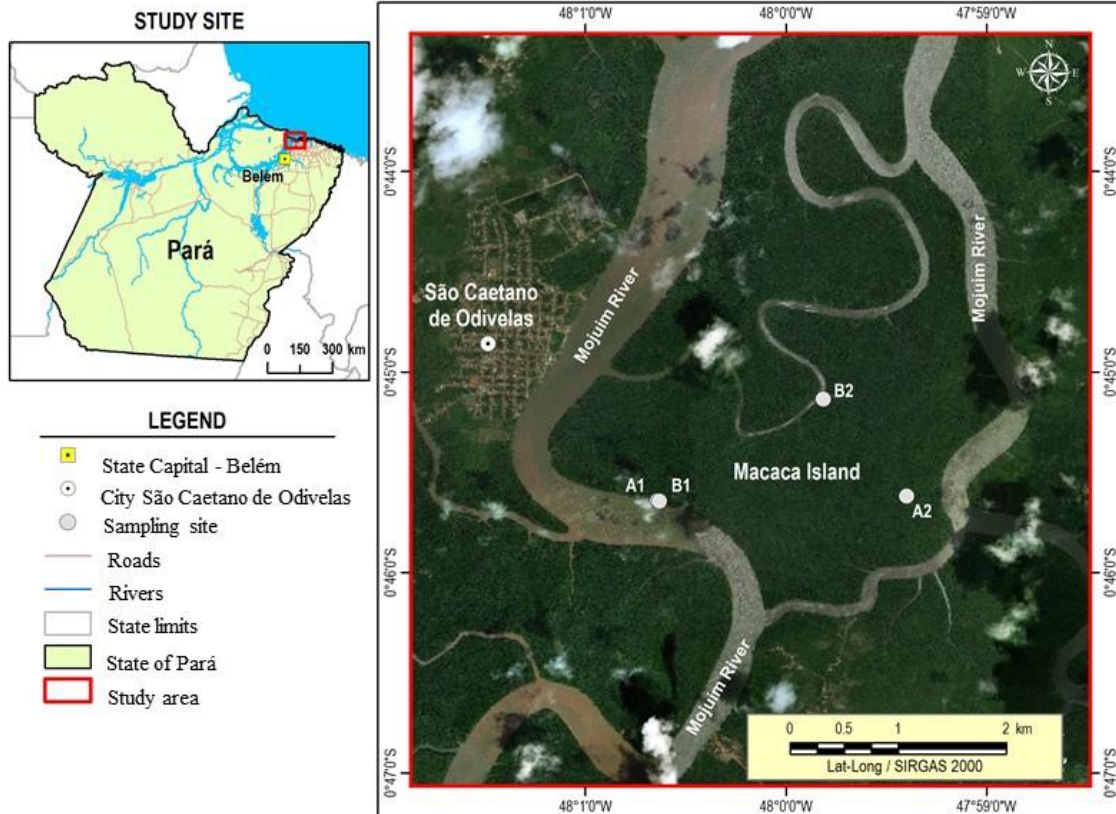
Figure 1. The Macaca Island located in the mangrove coast of Northern Brazil, Municipality of São Caetano de Odivelas (state of Pará), with sampling points at low (plot B1 and plot B2) and high topographies (plot A1 and plot A2). Image Source: © Google Earth

The Mojuim River region is geomorphologically formed by partially submerged river basins consequent of the increase in the relative sea level during the Holocene (Prost et al., 2001) associated with the formation of mangroves, dunes, and beaches (El-Robrini et al., 2006). This river forms the entire watershed of the municipality of São Caetano de Odivelas and borders the municipality of São João da Ponta (Figure 1). Before reaching the estuary, the Mojuim River crosses an area of a dryland forest highly fragmented by family farming, forming remnants of secondary forest (< 5.0 ha) of various ages (Fernandes and Pimentel, 2019). The population economically exploited the estuary, primarily by artisanal fishing, crab (*Ucides cordatus* L.) extraction, and oyster farms.

The flora of the mangrove area of Macaca Island is little anthropized and comprises the plant genera *Rhizophora*, *Avicenia*, *Laguncularia*, and *Acrostichum* (Ferreira, 2017; França et al., 2016). The estuarine plains are influenced by macrotide dynamics and can

4

be physiographically divided into four sectors (França et al., 2016). The Macaca Island is ranked as being from the fourth sector, which implies having woods of adult trees of the genus *Ryzophora* with an average height of 10 to 25 m, being located at an elevation of 0 to 5 m, and having silt-clay soil (França et al., 2016).

Four sampling plots were selected in the Macaca Island (Figure 1) on 19/05/2017, when the moon was in the waning quarter phase: two plots where flooding occurs every day (plots B1 and B2; Figure 1), called low topography (Top_Low), and two plots where flooding occurs only at high tides during the solstice and on the high tides of the rainy season of the new and full moons (plots A1 and A2; Figure 1), called high topography (Top_High).

2.2 Greenhouse gas flux measurements

In each plot, eight Polyvinyl Chloride rings with 0.20 m diameter and 0.12 m height were randomly installed within a circumference with a diameter of 20 m. The rings had an area of 0.028 m^{-2} (volume of 3.47 L), were fixed 0.05 m into the ground, and remained in place until the study was completed. Once a month, the Greenhouse gas flux was measured during periods of waning or crescent moon, as these are the times when the soil in the low topography is more exposed. To avoid the influence of mangrove roots on the gas fluxes, the rings were placed in locations without any seedlings or aboveground mangrove roots. CO_2 and CH_4 concentrations (ppm) were measured using the dynamic chamber methodology (Norman et al., 1997; Verchot et al., 2000), sequentially connected to a Los Gatos Research portable gas analyzer (Mahesh et al., 2015). The device was calibrated monthly with a high quality standard gas (500 ppm CO_2; 5 ppm CH_4). The rings were sequentially closed for three minutes with a PVC cap, being connected to the analyzer through two 12.0 m polyethylene hoses. The gas concentration was measured every two seconds and automatically stored by the analyzer. CO_2 and CH_4 fluxes were calculated from the linear regression of increasing/decreasing CO_2 and CH_4 concentrations within the chamber, usually between one and three minutes after the ring cover was placed (Frankignoulle, 1988; McEwing et al., 2015). The flux is considered zero when the linear regression reaches an $R^2 <$ 0.30 (Sundqvist et al., 2014). However, in our analyses, most regressions reached $R^2 >$ 0.70, and the regressions were weak and considered zero in only 6% of the samples. At the end of each flux measurement, the height of the ring above ground was measured at

144 four equidistant points with a ruler. The seasonal data were analyzed by comparing the

145 average monthly fluxes in the wet season and dry season separately.

146 2.3 Vegetation structure and biomass

147 The floristic survey was conducted in October 2017 using circular 1,256.6 m^2 plots

148 (Kauffman et al., 2013) divided into four 314.15 m^2 subplots, which is the equivalent to

149 0.38 ha (Figure 1), at the same topographies as the gas flux analysis. We recorded the

150 diameter above the aerial roots, the diameter of the stem, and total height of all trees

151 with DBH (diameter at breast height; m) greater than 0.05m. The allometric equations

152 (Howard et al., 2014) to calculate tree biomass (aboveground biomass; AGB) were:

153 $AGB = 0.1282 * DBH^{2.6}$ ($R^2 = 0.92$) for *R. mangle*; $AGB = 0.140 * DBH^{2.4}$ ($R^2 = 0.97$)

154 for *A. germinans*; and Total $AGB = 0.168 * \rho * DBH^{2.47}$ ($R^2 = 0.99$), where $\rho_{R.\ mangle} =$

155 0.87; $\rho_{A.\ germinans} = 0.72$ (ρ = wood density).

156 2.4 Soil sampling and environmental characterization

157 Four soil samples were collected with an auger at a depth of 0.10 m in all the studied

158 plots for gas flux measurements in July 2017 (beginning of the dry season) and January

159 2018 (beginning of the rainy season; Figure 1). Before the soil samples were removed,

160 pH and redox potential (Eh; mV) were measured with a Metrohm 744 equipment by

161 inserting the platinum probe directly into the intact soil at a depth of 0.10 m (Bauza et

162 al., 2002). The soil samples collected in the field were transported to the laboratory

163 (Chemical Analysis Laboratory of the *Museu Paraense Emílio Goeldi*) in thermal boxes

164 containing ice. The soil samples were analyzed on the day after collection at the

165 laboratory, and the samples were kept in a freezer. Salinity (Sal; ppt) was measured with

166 PCE-0100, and soil moisture (Sm; %) by the residual gravimetric method (EMBRAPA,

167 1997).

168 Organic Matter (OM; g kg^{-1}), Total Carbon (T_C; g kg^{-1}) and Total Nitrogen (T_N; g kg^{-1})

169 were calculated by volumetry (oxidoreduction) using the Walkley-Black method

170 (Kalembasa and Jenkinson, 1973). Microbial carbon (C_{mic}; mg kg^{-1}) and microbial

171 nitrogen (N_{mic}; mg kg^{-1}) were determined through the 2.0 min of Irradiation-extraction

172 method of soil by microwave technique (Islam and Weil, 1998). Microwave heated soil

173 extraction proved to be a simple, fast, accurate, reliable, and safe method to measure

174 soil microbial biomass (Araujo, 2010; Ferreira et al., 1999; Monz et al., 1991). The C_{mic}

175 was determined by dichromate oxidation (Kalembasa and Jenkinson, 1973; Vance et al.,

176 1987). The N_{mic} was analyzed following the method described by Brookes et al. (1985),

177 changing fumigation to irradiation, which uses the difference between the amount of T_N

178 in irradiated and non-irradiated soil. We used the flux conversion factor of 0.33

179 (Sparling and West, 1988) and 0.54 (Almeida et al., 2019; Brookes et al., 1985), for

180 carbon and nitrogen, respectively. Particle size analysis was performed separately on

181 four soil samples collected at each flux plot, in the two seasons (October 2017 and

182 March 2018), according to EMBRAPA (1997).

183 At each gas flux measurement, environmental variables such as air temperature (T_{air},

184 °C), relative humidity (RH, %), and wind speed (W_s, m s^{-1}) were quantified with a

185 portable thermo-hygrometer (model AK821) at the height of 2.0 m above the soil

186 surface. Soil temperature (T_s, °C) was measured with a portable digital thermometer

187 (model TP101) after each gas flux measurement. Daily precipitation was obtained from

188 an automatic precipitation station installed at a pier on the banks of the Mojuim River in

189 São Caetano das Odivelas (coordinates: -0.738333 latitude; -48.013056 longitude).

190 **2.5   Statistical analyses**

191 On the Macaca Island, two treatments were allocated (low and high topography), with

192 two plots in either. In each plot, eight chambers were randomly distributed, which were

193 considered sample repetitions. The normality of the data of FCH_4, FCO_2, and soil

194 physicochemical parameters was evaluated using the Shapiro-Wilks method. The soil

195 CO_2 and CH_4 flux showed a non-normal distribution. Therefore, we used the non-

196 parametric ANOVA (Kruskal-Wallis, $p < 0.05$) to test the differences between the two

197 treatments among months and seasons. The physicochemical parameters were normally

198 distributed. Therefore, a parametric ANOVA was used to test the statistical differences

199 ($p < 0.05$) between the two treatments among months and seasons. Pearson correlation

200 coefficients were calculated to determine the relationships between soil properties and

201 gas fluxes in the months (dry and wet season) when the chemical properties of the soil

202 were analyzed at the same time as gas fluxes were measured. Statistical analyses were

203 performed with the free statistical software Infostat 2015®.

204 **3   Results**

205 **3.1   Carbon dioxide and methane fluxes**

206 CO_2 fluxes differed significantly between topographies only in January (H = 3.915; p =

207 0.048), July (H = 9.091; p = 0.003), and November (H = 11.294; p < 0.000) (Figure 2;

208   Supplementary Information, SI 1), with generally higher fluxes at the high topography
209   than at the low topography. At the high topography, CO_2 fluxes were significantly
210   higher (H = 24.510; p = 0.011) in July compared to August and December, March,
211   October, and May, not differing from the other months of the year. Similarly, at the low
212   topography, CO_2 fluxes were statistically higher (H = 19.912; p = 0.046) in September
213   and February than in January and November, not differing from the other months. We
214   found a mean monthly flux of 327.9 ± 78.0 mg CO_2 m^{-2} h^{-1} (mean ± standard error) and
215   217.2 ± 51.0 mg CO_2 m^{-2} h^{-1} at the high and low topographies, respectively.
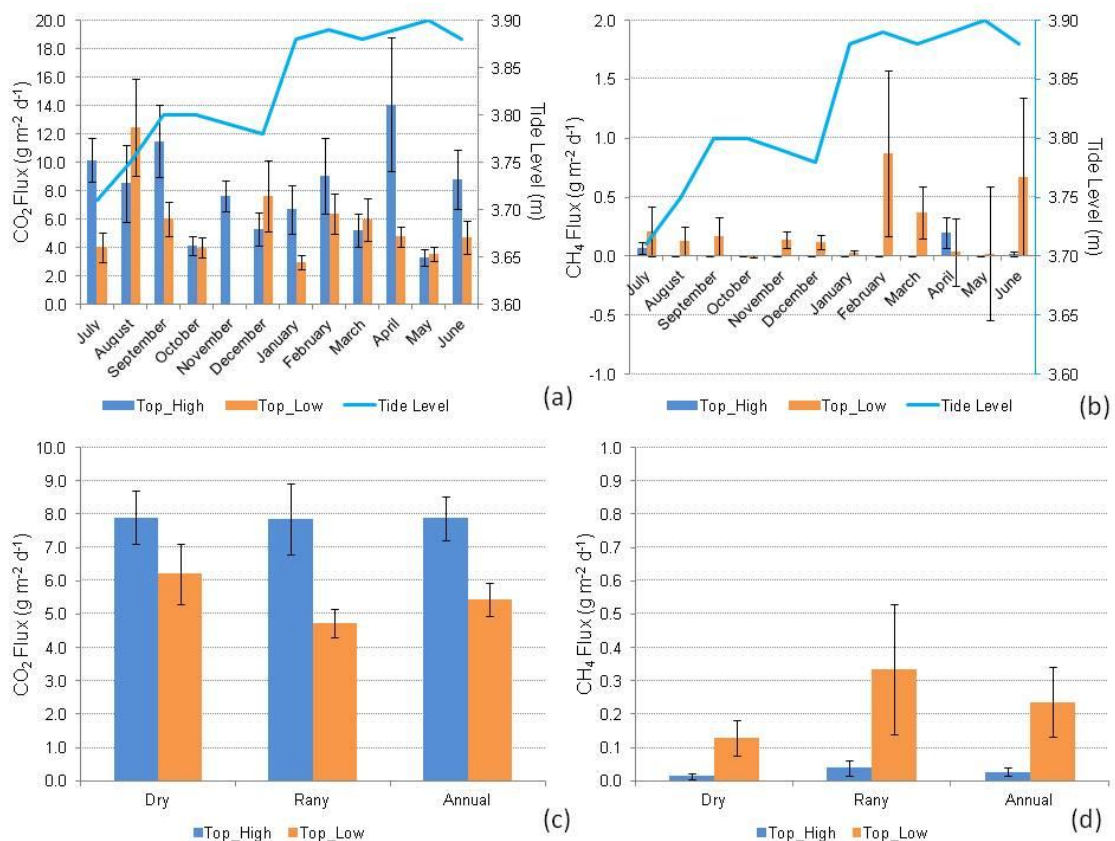
216

217   Figure 2. CO_2 (a) and CH_4 (b) fluxes (g CO_2 or CH_4 m^{-2} d^{-1}) monthly (July 2018 to June
218   2019) (n = 16). Seasonal (Dry and Rainy) and annual fluxes of CO_2 (c) and CH_4 (d), at
219   high (Top_High) and low (Top_Low) topographies (n = 96), in a mangrove forest soil
220   compared to tide level (Tide Level). The bars represent the standard error of the mean.

221   The CH_4 fluxes were statistically different between topographies only in November (H
222   = 9.276; p = 0.002) and December (H = 4.945; p = 0.005), with higher fluxes at the low
223   topography (Figure 2; SI 1). At the high topography, CH_4 fluxes were significantly (H =
224   40.073; p < 0.001) higher in April and July compared to the other months studied, and
225   in November CH_4 was consumed from the atmosphere (Figure 2; SI 1). Similarly, CH_4

226 fluxes at the low topography did not vary significantly among months (H = 10.114; p =
227 0.407).

228 Greenhouse gas fluxes (Figure 2) were only significantly different between
229 topographies in the dry season (Figure 3), period when CO_2 fluxes were higher (H =
230 7.378; p = 0.006) at the high topography and CH_4 fluxes at the low topography (H =
231 8.229; p < 0.001). In the Macaca Island, the mean annual fluxes of CO_2 and CH_4 were
232 6.659 ± 0.419 g CO_2 m^{-2} d^{-1} and 0.132 ± 0.053 g CH_4 m^{-2} d^{-1}, respectively.

233 **3.2   Weather data**

234 There was a marked seasonality during the study period (Figure 2), with 2,155.0 mm of
235 precipitation during the rainy period and 1,016.5 mm during the dry period. The highest
236 tides occurred in the period of greater precipitation (Figure 3) due to the rains. However,
237 the rainfall distribution was different from the climatological normal (Figure 3). The
238 precipitation in the rainy season was 553.2 mm below and in the dry season was 589.1
239 mm above the climatological normal. Thus, in the period studied, the dry season was
240 rainier and the rainy season drier than the climatological normal, which may be a
241 consequence of global climate change.

242

243
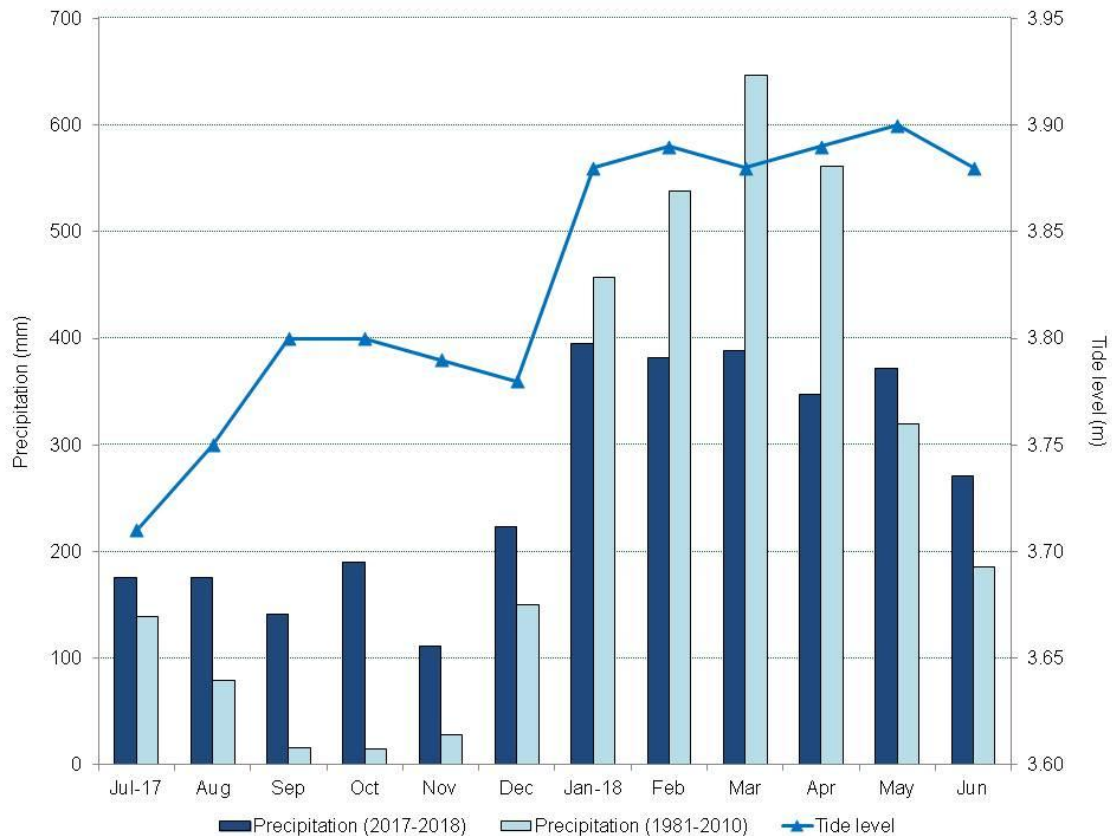
Figure 3. Monthly climatological normal in the municipality of Soure (1981-2010, mm), monthly precipitation (mm), and maximum tide height (m) from 2017 to 2018, in the municipality of São Caetano de Odivelas (PA).

T_{air} was significantly higher (LSD = 0.72, p = 0.01) at the high (31.24 ± 0.26 °C) than at the low topography (30.30 ± 0.25 °C) only in the rainy season (Figure 4a). No significant variation in T_s was found between topographies in either season (Figure 4b). RH was significantly higher (LSD = 2.55, p = 0.01) at the high topography (70.54 ± 0.97%) than at the low topography (66.85 ± 0.87%) only in the rainy season (Figure 4c). W_s (Figure 4d) was significantly higher (LSD = 0.15, p < 0.00) at the low (0.54 ± 0.06 m s^{-1}) than at the high topography (0.24 ± 0.04 m s^{-1}) also in the rainy season.
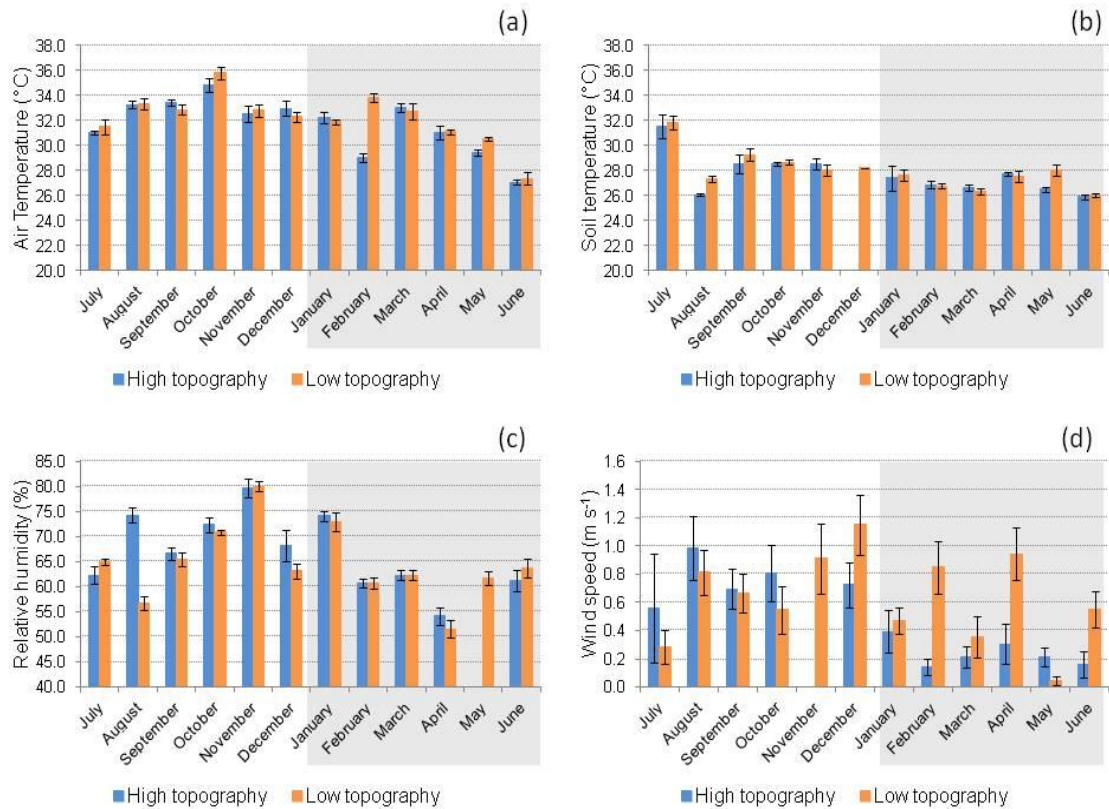
Figure 4. a) Air temperature (°C), b) soil temperature (°C), c) relative humidity (%), and d) wind speed (m s^{-1}) at high and low topographies, from July 2017 to June 2018 in a mangrove area in the Mojuim River estuary. Bars highlighted in grey correspond to the rainy season (n = 16). The bars represent the standard error.

3.3 Soil characteristics

Silt concentration was higher at the low topography (LSD: 14.763; p= 0.007) and clay concentration was higher at the high topography plots (LSD: 12.463; p= 0.005), in both seasons studied (Table 1). Soil particle size analysis did not differ statistically (p > 0.05) between the two seasons (Table 1). Soil moisture did not vary significantly (p > 0.05) between topographies at each season, or between seasonal periods at the same topography (Table 1). The pH varied statistically (LSD: 5.950; p= 0.006) only at the low topography when the two seasons were compared, being more acidic in the dry period (Table 1). The pH values were significantly (LSD: 0.559; p= 0.008) higher in the dry season (Table 1). No variation in Eh was identified between topographies and seasons (Table 1), although it was higher in the dry season than in the rainy season. However, Sal values were higher (LSD: 3.444; p = 0.010) at the high topography than at

271   the low topography in the dry season (Table 1). In addition, Sal was significantly higher

272   in the dry season than in the rainy season, in both high (LSD: 2.916; $p < 0.001$) and low

273   (LSD: 3.003; $p < 0.001$) topographies (Table 1). (Table 1).

Table 1. Analysis of Sand (%), Silt (%), Clay (%), Moisture (%), pH, Redox Potential (Eh, mV) and salinity (Sal; ppt) in the mangrove soil of high and low topographies, and in the rainy and dry seasons (Macaca island, São Caetano das Odivelas). Numbers represent the mean ± standard error of the mean. Lower case letters compare topographies in each seasonal period and upper-case letters compare the same topography between seasonal periods. Different letters indicate statistical difference (LSD, $p < 0.05$).

Season	Topography	Sand (%)	Silt (%)	Clay (%)	Moisture (%)	pH	Eh (mV)	Sal (ppt)
Dry	High	12.1±1.4[aA]	41.8±3.3[bA]	46.1±2.6[aA]	73.1±6.6[aA]	5.5±0.2[aA]	190.25±45.53[aA]	35.25±1.11[aA]
	Low	9.7±2.5[aA]	63.6±6.1[aA]	26.6±5.2[bA]	86.9±3.4[aA]	5.3±0.3[aA]	106.38±53.76[aA]	30.13±1.16[bA]
	Mean	10.9±1.4[A]	52.7±4.4[A]	36.4±3.8[A]	80.0±4.0[A]	5.4±0.2[A]	148.31±35.71[A]	32.69±1.02[A]
Rainy	High	12.1±1.4[aA]	41.8±3.3[bA]	46.1±2.6[aA]	88.9±3.5[aA]	4.9±0.4[aA]	92.50±56.20[aA]	7.50±0.78[aB]
	Low	9.7±2.5[aA]	63.6±6.1[aA]	26.6±5.2[bA]	88.6±3.7[aA]	4.4±0.1[aB]	36.25±49.97[aA]	8.13±0.79[aB]
	Mean	10.9±1.4[A]	52.7±4.4[A]	36.4±3.8[A]	88.7±2.5[A]	4.6±0.2[B]	64.38±37.04[A]	7.81±0.54[B]

279 The C_{mic} did not differ between topographies in the two seasons (Table 2). However, T_C

280 was significantly higher in the low topography in the dry season (LSD: 5.589; $p <$

281 0.000) and in the rainy season (LSD: 5.777; $p = 0.024$). In addition, C_{mic} was higher in

282 the dry season in both the high (LSD: 11.325; $p < 0.010$) and low (LSD: 9.345; $p <$

283 0.000) topographies (Table 2). N_{mic} did not vary between topographies seasonally.

284 However, N_{mic} in the high (LSD: 9.059; $p = 0.013$) and low topographies (LSD: 4.447;

285 $p = 0.001$) was higher during the dry season (Table 2). The C/N ratio (Table 2) was

286 higher in the low than in the high topography in both the dry (LSD: 3.142; $p < 0.000$)

287 and rainy seasons (LSD: 3.675; $p = 0.033$). However, only in the low topography was

288 the C/N ratio higher (LSD: 1.863; $p < 0.000$) in the dry season than in the rainy season

289 (Table 2). Soil OM was higher at the low topography in the rainy (LSD: 9.950; $p =$

290 0.024) and in the dry seasons (LSD: 9.630; $p < 0.000$). However, only in the lowland

291 topography was the OM concentration higher in the dry season than in the rainy season

292 (Table 2).

293 Table 2. Seasonal and topographic variation in microbial Carbon (C_{mic}; mg kg^{-1}), microbial Nitrogen (N_{mic}, mg kg^{-1}), Total Carbon (T_C; g kg^{-1}),

294 Total Nitrogen (N_T; g kg^{-1}), Carbon/Nitrogen ratio (C/N) and Soil Organic Matter (OM; g kg^{-1}). Numbers represent the mean (±standard error).

295 Lower case letters compare topographies at each season, and upper-case letters compare the topography between seasons.

Season	Topography	C_{mic} mg kg^{-1}	N_{mic} mg kg^{-1}	T_C g kg^{-1}	T_N g kg^{-1}	C/N	OM g kg^{-1}
	High	22.12±5.22^{aA}	12.76±4.20^{aA}	14.12±2.23^{bA}	1.43±0.06^{aA}	9.60±1.20^{bA}	24.35±3.84^{bA}
Dry	Low	26.34±4.23^{aA}	10.34±2.05^{aA}	26.44±1.35^{aA}	1.56±0.04^{aA}	16.98±0.84^{aA}	45.59±2.32^{aA}
	Mean	24.23±3.29 ^{A}	11.55±2.28 ^{A}	20.28 ±2.03 ^{A}	1.49±0.04 ^{A}	13.29±1.19^{A}	34.97±3.50 ^{A}
	High	7.40±0.79^{aB}	0.75±0.41^{aB}	11.46±2.48^{bA}	1.32±0.04^{aA}	8.42±1.70^{bA}	19.75±4.27^{bA}
Rainy	Low	5.95±1.06^{aB}	1.23±0.28^{aB}	18.27±1.06^{aB}	1.46±0.06^{aA}	12.47±0.22^{aB}	31.51±1.83^{aB}
	Mean	6.68±0.67 ^{B}	0.99±0.25 ^{B}	14.86 ±1.57 ^{B}	1.39±0.04 ^{A}	10.44±0.98^{A}	25.63±2.71 ^{B}

296

3.4 Vegetation structure and biomass

Only the species *R. mangle* and *A. germinans* were found in the floristic survey carried out. The DBH did not vary significantly between the topographies for either species (Table 3). However, *R. mangle* had a higher DBH than *A. germinaris* at both high (LSD: 139.304; p = 0.037) and low topographies (LSD: 131.307; p = 0.001). The basal area (BA) and AGB did not show significant variation (Table 3). A total aboveground biomass of 322.1 ± 49.6 Mg ha^{-1} was estimated.

305 Table 3: Summed Diameter at Breast Height (DBH; cm), Basal Area (BA; m^2 ha^{-1}) and Aboveground Biomass (AGB; Mg ha^{-1}) at high and low
306 topographies in the mangrove forest of the Mojuim River estuary. Numbers represent the mean ± standard error of the mean. Lower case letters
307 compare topographic height for each species, and upper-case letters compare species at each topographic height, using Tukey's test ($p < 0.05$).

Specie	Topography	N ha^{-1}	DBH (cm)	BA (m^2 ha^{-1})	AGB (Mg ha^{-1})
Rhizophora mangle	High	302.4±20.5	238.8±24.9[aA]	17.3±2.0[aA]	219.3±25.7[aA]
	Low	310.4±37.6	283.5±45.0[aA]	24.2±4.3[aA]	338.7±62.9[aA]
Avicennia germinans	High	47.7±20.5	86.8±51.2[aB]	13.8±9.2[aA]	135.3±94.7[aA]
	Low	15.9±9.2	46.1±29.3[aB]	11.8±8.8[aA]	136.0±108.3[aA]
Total	High	350.2±18.4	325.6±33.6[a]	31.1±7.5[a]	304.5±99.8[a]
	Low	346.2±41.0	296.0±23.7[a]	30.0±4.1[a]	330.8±60.4[a]

308 The equations for biomass estimates (AGB) were: *R. mangle* = $0.1282 \ast DBH^{2.6}$; *A. germinans* = $0.14 \ast DBH^{2.4}$; and Total = $0.168 \ast \rho \ast DBH^{2.47}$, where $\rho_{R. mangle}$ = 0.87; $\rho_{A. germinans}$
309 = 0.72 (Howard et al., 2014).

310

3.5   Drivers of greenhouse gas fluxes

In the rainy season, CO_2 efflux was correlated with T_{air} (Pearson = 0.23, p = 0.03), RH (Pearson = -0.32, p < 0.00) and T_s (Pearson = 0.21, p = 0.04) only at the low topography. In the dry season CO_2 flux was correlated with T_s (Pearson = 0.39, p < 0.00) at the low topography. The dry season was the period in which we found the greatest amount of significant correlations between CO_2 efflux and soil chemical parameters, while the C:N ratio, OM, and Eh were correlated with CO_2 efflux in both seasons (Table 4). The negative correlation between T_C, N_T, C/N, and OM, along with the positive correlation of N_{mic} with soil CO_2 flux, in the dry period, indicates that microbial activity is a decisive factor for CO_2 efflux (Table 4). Soil moisture in the Mojuim River mangrove forest negatively influenced CO_2 flux in both seasons (Table 4). However, soil moisture was not correlated with CH_4 flux. No significant correlations were found between CH_4 efflux and the chemical properties of the soil in the mangrove of the Mojuim River estuary (Table 4). However, more detailed studies on CH_4 efflux and on its relationship with methanotrophic bacteria and abiotic factors (mainly ammonia and sulfate) are needed due to the average flux of 4.70 mg C m^{-2} h^{-1} and the extreme monthly and seasonal variations.

328

329 Table 4. Correlation coefficient (Pearson) of CO_2 and CH_4 fluxes with chemical parameters of the soil in a mangrove area in the Mojuim River

330 estuary.

Gas Flux ($g\ m^{-2}\ d^{-1}$)	Season	T_C ($g\ kg^{-1}$)	T_N ($g\ kg^{-1}$)	C_{mic} ($mg\ kg^{-1}$)	N_{mic} ($mg\ kg^{-1}$)	C/N	OM ($g\ kg^{-1}$)	Sal (ppt)	Eh (mV)	pH	Moisture (%)
	Dry	-0.68^{**}	-0.59^{*}	0.18^{NS}	0.61^{**}	-0.66^{**}	-0.67^{**}	-0.07^{NS}	0.51^{*}	0.21^{NS}	-0.49^{*}
CO_2	Rainy	-0.44^{NS}	-0.20^{NS}	-0.15^{NS}	-0.32^{NS}	-0.50^{*}	-0.63^{**}	-0.54^{*}	0.53^{*}	0.47^{NS}	-0.54^{*}
	Annual	-0.50^{**}	-0.35^{*}	-0.18^{NS}	0.00^{NS}	-0.53^{**}	-0.48^{**}	-0.30^{NS}	0.39^{*}	0.23^{NS}	-0.56^{**}
	Dry	0.30^{NS}	0.07^{NS}	-0.14^{NS}	-0.24^{NS}	0.34^{NS}	0.02^{NS}	-0.04^{NS}	-0.38^{NS}	0.26^{NS}	0.26^{NS}
CH_4	Rainy	0.05^{NS}	-0.09^{NS}	0.44^{NS}	-0.27^{NS}	0.09^{NS}	-0.11^{NS}	-0.04^{NS}	-0.13^{NS}	-0.07^{NS}	0.04^{NS}
	Annual	0.04^{NS}	-0.10^{NS}	-0.01^{NS}	-0.18^{NS}	0.08^{NS}	-0.01^{NS}	-0.17^{NS}	-0.21^{NS}	-0.08^{NS}	0.02^{NS}

331 Total Carbon (T_C; $g\ kg^{-1}$); Total Nitrogen (T_N; $g\ kg^{-1}$); Microbial Carbon (Cmic, $g\ kg^{-1}$); Microbial Nitrogen (N_{mic}, $g\ kg^{-1}$); Carbon and Nitrogen

332 ratio (C/N); Organic Matter (OM; $g\ kg^{-1}$); Salinity (Sal; ppt); Redox Potential (Eh; mV); Soil Moisture (Moisture, %).

333 NS= not significant; * significant effects at $p \le 0.05$; ** significant effects at $p \le 0.01$

334

4   Discussion

4.1   Carbon dioxide and methane flux

It is important to consider that the year under study was rainier in the dry season (2017) and less rainy in the wet season (2018) when the climatological average is concerned (1981-2010) (Figure 3). Perhaps this variation is related to the effects of global climate changes. Under these conditions, negative and positive flows of the two greenhouse gases were found (negative values represent gas consumption) Under these conditions, the CO_2 flux from the mangrove soil ranged from -5.06 to 68.96 g CO_2 m^{-2} d^{-1} (mean 6.66 g CO_2 m^{-2} d^{-1}), while the CH_4 flux ranged from -5.07 to 11.08 g CH_4 m^{-2} d^{-1} (mean 0.13 g CH_4 m^{-2} d^{-1}), resulting in a total carbon rate of 1.92 g C m^{-2} d^{-1} or 7.00 Mg C ha^{-1} y^{-1} (Figure 2). The negative CO_2 flux is apparently a consequence of the increased CO_2 solubility in tidal waters or of the increased sulfate reduction, as described in the literature (Borges et al., 2018; Chowdhury et al., 2018; Nóbrega et al., 2016). Fluctuations in redox potential altered the availability of the terminal electron acceptor and donor, and the forces of recovery of their concentrations in the soil, such that a disproportionate release of CO_2 can result from the alternative anaerobic degradation processes such as sulfate and iron reduction (Chowdhury et al., 2018). The soil carbon flux in the mangrove area in the Amazon region was within the range of findings for other tropical mangrove areas (2.57 to 11.00 g CO_2 m^{-2} d^{-1}; Shiau and Chiu, 2020). However, the mean flux of 6.2 mmol CO_2 m^{-2} h^{-1} recorded in this Amazonian mangrove was much higher than the mean efflux of 2.9 mmol CO_2 m^{-2} h^{-1} recorded in 75 mangroves during low tide periods (Alongi, 2009).

An emission of 0.010 Tg CH_4 y^{-1}, 0.64 g CH_4 m^{-2} d^{-1} (Rosentreter et al., 2018a), or 26.7 mg CH_4 m^{-2} h^{-1} has been reported for tropical latitudes (0 and 5°). In our study, the monthly average of CH_4 flux was higher at the low (7.3 ± 8.0 mg CH_4 m^{-2} h^{-1}) than at the high topography (0.9 ± 0.6 mg C m^{-2} h^{-1}), resulting in 0.13 g CH_4 m^{-2} d^{-1} or 0.48 Mg CH_4 ha^{-1} y^{-1} (Figure 2). Therefore, the CH_4-C fluxes from the mangrove soil in the Mojuim River estuary were much lower than expected. It is known that there is a microbial functional module for CH_4 production and consumption (Xu et al., 2015) and diffusibility (Sihi et al., 2018), and considers three key mechanisms: aceticlastic methanogenesis (acetate production), hydrogenotrophic methanogenesis (H_2 and CO_2 production), and aerobic methanotrophy (CH_4 oxidation and O_2 reduction). The average emission from the soil of 8.4 mmol CH_4 m^{-2} d^{-1} was well below the fluxes recorded in

368   the Bay of Bengal, with 18.4 mmol CH_4 m^{-2} d^{-1} (Biswas et al., 2007). In the Amazonian

369   mangrove studied the mean annual carbon equivalent efflux was 429.6 mg CO_{2-eq} m^{-2} h^{-1}

370   . This value is 0.00004% of the erosion losses of 103.5 Tg CO_{2-eq} ha^{-1} y^{-1} projected for

371   the next century in tropical mangrove forests (Adame et al., 2021). These higher CO_2

372   flux concomitantly with lower CH_4 flux in this Amazonian estuary are probably a

373   consequence of changes in the rainfall pattern already underway, where the dry season

374   was wetter and the rainy season drier when compared to the climatological normal.

375   **4.2   Drivers of greenhouse gas fluxes**

376   Mangrove areas are periodically flooded, with a larger flood volume during the syzygy

377   tides, especially in the rainy season. The hydrological condition of the soil is determined

378   by the microtopography and can regulate the respiration of microorganisms (aerobic or

379   anaerobic), being a decisive factor in controlling the CO_2 efflux (Dai et al., 2012;

380   Davidson et al., 2000; Ehrenfeld, 1995). In the two climatic periods of the year, the high

381   topography produced more CO_2 (7.869 ± 1.873 g CO_2 m^{-2} d^{-1}) than the low topography

382   (5.212 ± 1.225 g CO_2 m^{-2} d^{-1}) (Figure 2; SI 1). No significant influence on CO_2 flux was

383   observed due to the low variation in high tide level throughout the year (0.19 m) (Figure

384   2), although it was numerically higher at the high topography. However, tidal height

385   and the rainy season resulted in a higher CO_2 flux (rate high/low =1.7) at the high

386   topography (7.858 ± 0.039 g CO_2 m^{-2} d^{-1}) than at the low topography (4.734 ± 0.335 g

387   CO_2 m^{-2} d^{-1}) (Figure 2; SI 1). This result is because the root systems of most flood-

388   tolerant plants remain active when flooded (Angelov et al., 1996). Still, the high

389   topography has longer flood-free periods, which only happens when the tides are

390   syzygy or when the rains are torrential.

391   CO_2 efflux was higher in the high topography than in the low topography in the rainy

392   season (when soils are more subject to inundation), i.e., 39.8% lower in the forest soil

393   exposed to the atmosphere for less time. Measurements performed on 62 mangrove

394   forest soils showed an average flux of 2.87 mmol CO_2 m^{-2} h^{-1} when the soil was

395   exposed to the atmosphere, while 75 results on flooded mangrove forest soils showed an

396   average emission of 2.06 mmol CO_2 m^{-2} h^{-1} (Alongi, 2007, 2009), i.e., 28.2% less than

397   for the dry soil. This reflects the increased facility gases have for molecular diffusion

398   than fluids, and the increased surface area available for aerobic respiration and chemical

399   oxidation during air exposure (Chen et al., 2010). Some studies attribute this variation

400   to the temperature of the soil when it is exposed to tropical air (Alongi, 2009), which

401   increases the export of dissolved inorganic carbon (Maher et al., 2018). However,

402   although despite the lack of significant variation in soil temperature between

403   topographies at each time of year (Figure 4b), there was a positive correlation (Pearson

404   = 0.15, p = 0.05) between CO_2 efflux and soil temperature at the low topography.

405   Some studies show that CH_4 efflux is a consequence of the seasonal temperature

406   variation in mangrove forest under temperate/monsoon climates (Chauhan et al., 2015;

407   Purvaja and Ramesh, 2001; Whalen, 2005). However, in your study CH_4 efflux was

408   correlated with Ta (Pearson = -0.33, p < 0.00) and RH (Pearson = 0.28, p = 0.01) only

409   in the dry season and at the low topography. The results show that the physical

410   parameters do not affect the fluxes in a standardized way, and their greater or lesser

411   influence depends on the topography and seasonality.

412   A compilation of several studies showed that the total CH_4 emissions from the soil in a

413   mangrove ecosystem range from 0 to 23.68 mg C m^{-2} h^{-1} (Shiau and Chiu, 2020), and

414   our study showed a range of -0.01 to 31.88 mg C m^{-2} h^{-1} (mean of 4.70 ± 5.00 mg C m^{-2}

415   h^{-1}). The monthly CH_4 fluxes were generally higher at the low (0.232 ± 0.256) than at

416   the high (0.026 ± 0.018) topography, especially during the rainy season when the tides

417   were higher (Figure 2). Only in the dry season was there a significantly higher

418   production at the low than at the high topography (Figure 2; SI 1). The low topography

419   produced 0.0249 g C m^{-2} h^{-1} more to the atmosphere in the rainy season than in the dry

420   season (Figure 2), and a similar seasonal pattern was recorded in other studies

421   (Cameron et al., 2021).

422   The mangrove soil in the Mojuim River estuary is rich in silt and clay (Table 1), which

423   reduces sediment porosity and fosters the formation and maintenance of anoxic

424   conditions (Dutta et al., 2013). In addition, the lack of oxygen in the flooded mangrove

425   soil favors microbial processes such as denitrification, sulfate reduction,

426   methanogenesis, and redox reactions (Alongi and Christoffersen, 1992). A significant

427   amount of CH_4 produced in wetlands is dissolved in the pore water due to high pressure,

428   causing supersaturation, which allows CH_4 to be released by diffusion from the

429   sediment to the atmosphere and by boiling through the formation of bubbles.

430   Studies show that the CO_2 flux tends to be lower with high soil saturation (Chanda et

431   al., 2014; Kristensen et al., 2008). A total of 395 Mg C ha^{-1} was found at the soil surface

432   (0.15 m) in the mangrove of the Mojuim River estuary, which was slightly higher than

433   the 340 Mg C ha^{-1} found in other mangroves in the Amazon (Kauffman et al., 2018),

434 however being significantly 1.8 times greater at the low topography (Table 2). The finer

435 soil texture at the low topography (Table 1) reduces groundwater drainage which

436 facilitates the accumulation of C in the soil (Schmidt et al., 2011).

4.3 Mangrove biomass

438 Only the species *R. mangle* and *A. germinans* were found in the floristic survey carried

439 out, which is aligned with the results of other studies in the same region (Menezes et al.,

440 2008). Thus, the variations found in the flux between the topographies in the Mojuim

441 River estuary are not related to the mangrove forest structure, because there was no

442 difference in the aboveground biomass. Since there was no difference in the species

443 composition, the belowground biomass is not expected to differ either (Table 3).

444 Assuming that the amount of carbon stored is 0.42 of the total biomass (Sahu and

445 Kathiresan, 2019), the mangrove forest biomass of the Mojuim River estuary stores

446 127.9 and 138.9 Mg C ha^{-1} at the high and low topographies, respectively. This result is

447 well below the 507.8 Mg C ha^{-1} estimated for Brazilian mangroves (Hamilton and

448 Friess, 2018), but are near the 103.7 Mg C ha^{-1} estimated for a mangrove at Guará's

449 island (Salum et al., 2020), 108.4 Mg C ha^{-1} for the Bragantina region (Gardunho,

450 2017), and 132.3 Mg C ha^{-1} in French Guiana (Fromard et al., 1998). The biomass

451 found in the Mojuim estuary does not differ from the biomass found in other

452 Amazonian mangroves, despite being much lower than that found in other Brazilian

453 mangroves. The estimated primary production for tropical mangrove forests is 218 ± 72

454 Tg C y (Bouillon et al., 2008).

4.4 Biogeochemical parameters

456 During the seasonal and annual periods, CH_4 efflux was not significantly correlated

457 with chemical parameters (Table 5), which is similar to the observed in another study

458 (Chen et al., 2010). Flooded soils present reduced gas diffusion rates, which directly

459 affects the physiological state and activity of microbes, by limiting the supply of the

460 dominant electron acceptors (e.g., oxygen), and gases (e.g., CH_4) (Blagodatsky and

461 Smith, 2012). The importance of soil moisture was evident in the richness and diversity

462 of bacterial communities in a study that compared the different pore spaces filled with

463 water (Banerjee et al., 2016). Furthermore, sulfate reduction in flooded soils (another

464 pathway of organic matter metabolism) is dependent on the redox potential of the soil.

465 However, no sulfate reduction occurs when the redox potential has values are above -

466 150 mv (Connell and Patrick, 1968). In our study, Eh was above 36.0 mV indicating

467 that sulfate reduction probably did not influence the OM metabolism.

468 On the other hand, increasing soil moisture provides the microorganisms with essential

469 substrates such as ammonium, nitrate, and soluble organic carbon, and increases gas

470 diffusion rates in the water (Blagodatsky and Smith, 2012). Biologically available

471 nitrogen often limit marine productivity (Bertics et al., 2010), and thus can affect CO_2

472 fluxes to the atmosphere. However, a mangrove fertilization experiment showed that

473 CH_4 emission rates were not affected by N addition (Kreuzwieser et al., 2003). A higher

474 concentration of C_{mic} and N_{mic} in the dry period (Table 2), both in the high and low

475 topographies, indicated that microorganisms are more active when the soil spends more

476 time aerated in the dry period (Table 2), period when only the high tides produce anoxia

477 in the mangrove soil mainly in the low topography. Under reduced oxygen conditions,

478 in a laboratory incubated mangrove soil, the addition of nitrogen resulted in a

479 significant increase in the microbial metabolic quotient, showing no concomitant

480 change in microbial respiration, which was explained by a decrease in microbial

481 biomass (Craig et al., 2021).

482 The high OM concentration at the two topographic heights (Table 2), at the two seasons

483 studied, and the respective negative correlation with CO_2 flux (Table 5) confirm the

484 importance of microbial activity in mangrove soils (Gao et al., 2020). Also, CH_4

485 produced in flooded soils can be converted mainly to CO_2 by the anaerobic oxidation of

486 CH_4 (Boetius et al., 2000; Milucka et al., 2015; Xu et al., 2015) which may contribute to

487 the higher CO_2 efflux in the Mojuim River estuary compared to other tropical

488 mangroves (Rosentreter et al., 2018b). The belowground C stock is considered the

489 largest C reservoir in a mangrove ecosystem, and it results from the low OM

490 decomposition rate due to flooding (Marchand, 2017).

491 The higher water salinity influenced by the tidal movement in the dry season (Table 1)

492 seems to result in a lower CH_4 flux at the low topography (Dutta et al., 2013; Lekphet et

493 al., 2005; Shiau and Chiu, 2020). Sulfate (SO_4^{2-}) in the brine affects the competition

494 between SO_4^{2-} reduction and methanogenic fermentation, as sulfate-reducing bacteria

495 are more efficient at using hydrogen than methanotrophic bacteria (Abram and Nedwell,

496 1978; Kristjansson et al., 1982), a key factor fostering reduced CH_4 emissions. At high

497 SO_4^{2-} concentrations methanotrophic bacteria use CH_4 as an energy source and oxidize

498 it to CO_2 (Coyne, 1999; Segarra et al., 2015), increasing the efflux of CO_2 and reduced

499   CH_4 (Megonigal and Schlesinger, 2002; Roslev and King, 1996). This may explain the

500   high CO_2 efflux found throughout the year at the high and, especially, at the low

501   topographies (Figure 3).

502   Studies in coastal ecosystems in Taiwan have reported that methanotrophic bacteria can

503   be sensitive to soil pH, and reported an optimal growth at pH ranging from 6.5 to 7.5

504   (Shiau et al., 2018). The higher soil acidity in the Mojuim River wetland (Table 1) may

505   be inhibiting the activity of methanogenic bacteria by increasing the population of

506   methanotrophic bacteria, which are efficient in CH_4 consumption (Chen et al., 2010;

507   Hegde et al., 2003; Shiau and Chiu, 2020). In addition, the pneumatophores present in

508   *R. mangle* increase soil aeration and reduce CH_4 emissions (Allen et al., 2011; He et al.,

509   2019). Spatial differences (topography) in CH_4 emissions in the soil can be attributed to

510   substrate heterogeneity, salinity, and the abundance of methanogenic and

511   methanotrophic bacteria (Gao et al., 2020). The high Eh values found in both

512   topographies, mainly in the dry period (Table 1), hinder CH_4 emission. Soil Eh above -

513   150 mV has been considered limiting for CH_4 production (Yang and Chang, 1998).

514   Increases in CH_4 efflux with reduced salinity were found as a consequence of intense

515   oxidation or reduced competition from the more energetically efficient SO_4^{2-} and NO^{3-}

516   reducing bacteria when compared to the methanogenic bacteria (Biswas et al., 2007).

517   This fact can be observed in the CH_4 efflux in the mangrove of the Mojuim River,

518   because there was an increased CH_4 production especially in the low topography in the

519   rainy season (Figure 3), when water salinity is reduced (Table 1) due to the increased

520   precipitation. However, we did not find a correlation between CH_4 efflux and salinity,

521   as previously reported (Purvaja and Ramesh, 2001)

522   5   Conclusions

523   The most recent estimate between latitude 0° to 23.5° S shows an emission of 2.3 g CO_2

524   m^{-2} d^{-1} (Rosentreter et al., 2018b). However, the efflux in the mangrove of the Mojuim

525   River estuary was 6.7 g CO_2 m^{-2} d^{-1}. For the same latitudinal range, Rosentreter et al.

526   (2018c) estimated an emission of 0.64 g CH_4 m^{-2} d^{-1}, and we found an efflux of 0.13 g

527   CH_4 m^{-2} d^{-1}. Seasonality was important for CH_4 efflux but did not influence CO_2 efflux.

528   The differences in fluxes may be an effect of global climate changes on the terrestrial

529   biogeochemistry at the plant-soil-atmosphere interface, as indicated by the deviation in

530   precipitation values from the climatology normal, making it necessary to extend this

531   study for more years. Using the factor of 23 to convert the global warming potential of

532   CH_4 to CO_2 (IPCC, 2001), the CO_2 equivalent emission was 35.4 Mg $CO_{2\text{-eq}}$ ha^{-1} yr^{-1}.

533   Over a 100-year time period, a radiative forcing due to the continuous emission of 0.05

534   kg CH_4 m^{-2} y^{-1}found in this study, would be offset if CO_2 sequestration rates were 2.16

535   kg CO_2 m^{-2} y^{-1} (Neubauer and Megonigal, 2015).

536   Microtopography should be considered when determining the efflux of CO_2 and CH_4 in

537   mangrove forests in an Amazon estuary. The low topography in the mangrove forest of

538   Mojuim River had a higher concentration of organic carbon in the soil. However, it did

539   not produce a higher CO_2 efflux because it was negatively influenced by soil moisture,

540   which was indifferent to CH_4 efflux. MO, C/N ratio, and Eh were critical in soil

541   microbial activity, which resulted in a variation in CO_2 flux during the year and

542   seasonal periods. Thus, the physicochemical properties of the soil are important for CO_2

543   flux, especially in the rainy season. Still, they did not influence CH_4 fluxes.

559   **6   References**

560   Abram, J. W. and Nedwell, D. B.: Inhibition of methanogenesis by sulphate reducing

561   bacteria competing for transferred hydrogen, Arch. Microbiol., 117(1), 89–92,

562   doi:10.1007/BF00689356, 1978.

563 Adame, M. F., Connolly, R. M., Turschwell, M. P., Lovelock, C. E., Fatoyinbo, T.,
564 Lagomasino, D., Goldberg, L. A., Holdorf, J., Friess, D. A., Sasmito, S. D., Sanderman,
565 J., Sievers, M., Buelow, C., Kauffman, J. B., Bryan-Brown, D. and Brown, C. J.: Future
566 carbon emissions from global mangrove forest loss, Glob. Chang. Biol., 27(12), 2856–
567 2866, doi:10.1111/gcb.15571, 2021.

568 Allen, D., Dalal, R. C., Rennenberg, H. and Schmidt, S.: Seasonal variation in nitrous
569 oxide and methane emissions from subtropical estuary and coastal mangrove sediments,
570 Australia, Plant Biol., 13(1), 126–133, doi:10.1111/j.1438-8677.2010.00331.x, 2011.

571 Almeida, R. F. de, Mikhael, J. E. R., Franco, F. O., Santana, L. M. F. and Wendling, B.:
572 Measuring the labile and recalcitrant pools of carbon and nitrogen in forested and
573 agricultural soils: A study under tropical conditions, Forests, 10(7), 544,
574 doi:10.3390/f10070544, 2019.

575 Alongi, D. M.: The contribution of mangrove ecosystems to global carbon cycling and
576 greenhouse gas emissions, in Greenhouse gas and carbon balances in mangrove coastal
577 ecosystems, edited by Y. Tateda, R. Upstill-Goddard, T. Goreau, D. M. Alongi, A.
578 Nose, E. Kristensen, and G. Wattayakorn, pp. 1–10, Gendai Tosho, Kanagawa, Japan.,
579 2007.

580 Alongi, D. M.: The energetics of mangrove forests, Springer., 2009.

581 Alongi, D. M. and Christoffersen, P.: Benthic infauna and organism-sediment relations
582 in a shallow, tropical coastal area: influence of outwelled mangrove detritus and
583 physical disturbance, Mar. Ecol. Prog. Ser., 81(3), 229–245, doi:10.3354/meps081229,
584 1992.

585 Alongi, D. M. and Mukhopadhyay, S. K.: Contribution of mangroves to coastal carbon
586 cycling in low latitude seas, Agric. For. Meteorol., 213, 266–272,
587 doi:10.1016/j.agrformet.2014.10.005, 2015.

588 Angelov, M. N., Sung, S. J. S., Doong, R. Lou, Harms, W. R., Kormanik, P. P. and
589 Black, C. C.: Long-and short-term flooding effects on survival and sink-source
590 relationships of swamp-adapted tree species, Tree Physiol., 16(4), 477–484,
591 doi:10.1093/treephys/16.5.477, 1996.

592 Araujo, A. S. F. de: Is the microwave irradiation a suitable method for measuring soil
593 microbial biomass?, Rev. Environ. Sci. Biotechnol., 9(4), 317–321,

594 doi:10.1007/s11157-010-9210-y, 2010.

595 Banerjee, S., Helgason, B., Wang, L., Winsley, T., Ferrari, B. C. and Siciliano, S. D.:
596 Legacy effects of soil moisture on microbial community structure and N2O emissions,
597 Soil Biol. Biochem., 95, 40–50, doi:10.1016/j.soilbio.2015.12.004, 2016.

598 Bastviken, D., Tranvik, L. J., Downing, J. A., Crill, P. M. and Enrich-Prast, A.:
599 Freshwater Methane Emissions Offset the Continental Carbon Sink, Science (80-.).,
600 331(6013), 50–50, doi:10.1126/science.1196808, 2011.

601 Bauza, J. F., Morell, J. M. and Corredor, J. E.: Biogeochemistry of Nitrous Oxide
602 Production in the Red Mangrove (Rhizophora mangle) Forest Sediments, Estuar. Coast.
603 Shelf Sci., 55(5), 697–704, doi:10.1006/ECSS.2001.0913, 2002.

604 Bertics, V. J., Sohm, J. A., Treude, T., Chow, C. E. T., Capone, D. G., Fuhrman, J. A.
605 and Ziebis, W.: Burrowing deeper into benthic nitrogen cycling: The impact of
606 Bioturbation on nitrogen fixation coupled to sulfate reduction, Mar. Ecol. Prog. Ser.,
607 409, 1–15, doi:10.3354/meps08639, 2010.

608 Biswas, H., Mukhopadhyay, S. K., Sen, S. and Jana, T. K.: Spatial and temporal
609 patterns of methane dynamics in the tropical mangrove dominated estuary, NE coast of
610 Bay of Bengal, India, J. Mar. Syst., 68(1–2), 55–64, doi:10.1016/j.jmarsys.2006.11.001,
611 2007.

612 Blagodatsky, S. and Smith, P.: Soil physics meets soil biology: Towards better
613 mechanistic prediction of greenhouse gas emissions from soil, Soil Biol. Biochem., 47,
614 78–92, doi:10.1016/J.SOILBIO.2011.12.015, 2012.

615 Boetius, A., Ravenschlag, K., Schubert, C. J., Rickert, D., Widdel, F., Gleseke, A.,
616 Amann, R., Jørgensen, B. B., Witte, U. and Pfannkuche, O.: A marine microbial
617 consortium apparently mediating anaerobic oxidation methane, Nature, 407(6804), 623–
618 626, doi:10.1038/35036572, 2000.

619 Borges, A. V., Abril, G., Darchambeau, F., Teodoru, C. R., Deborde, J., Vidal, L. O.,
620 Lambert, T. and Bouillon, S.: Divergent biophysical controls of aquatic CO2 and CH4
621 in the World's two largest rivers, Sci. Rep., 5, doi:10.1038/srep15614, 2015.

622 Borges, A. V., Abril, G. and Bouillon, S.: Carbon dynamics and CO2 and CH4
623 outgassing in the Mekong delta, Biogeosciences, 15(4), doi:10.5194/bg-15-1093-2018,
624 2018.

625   Bouillon, S., Borges, A. V., Castañeda-Moya, E., Diele, K., Dittmar, T., Duke, N. C.,

626   Kristensen, E., Lee, S. Y., Marchand, C., Middelburg, J. J., Rivera-Monroy, V. H.,

627   Smith, T. J. and Twilley, R. R.: Mangrove production and carbon sinks: A revision of

628   global budget estimates, Global Biogeochem. Cycles, 22(2),

629   doi:10.1029/2007GB003052, 2008.

630   Brookes, P. C., Landman, A., Pruden, G. and Jenkinson, D. S.: Chloroform fumigation

631   and the release of soil nitrogen: A rapid direct extraction method to measure microbial

632   biomass nitrogen in soil, Soil Biol. Biochem., 17(6), 837–842, doi:10.1016/0038-

633   0717(85)90144-0, 1985.

634   Cameron, C., Hutley, L. B., Munksgaard, N. C., Phan, S., Aung, T., Thinn, T., Aye, W.

635   M. and Lovelock, C. E.: Impact of an extreme monsoon on CO_2 and CH_4 fluxes from

636   mangrove soils of the Ayeyarwady Delta, Myanmar, Sci. Total Environ., 760, 143422,

637   doi:10.1016/j.scitotenv.2020.143422, 2021.

638   Castillo, J. A. A., Apan, A. A., Maraseni, T. N. and Salmo, S. G.: Soil greenhouse gas

639   fluxes in tropical mangrove forests and in land uses on deforested mangrove lands,

640   Catena, 159, 60–69, doi:10.1016/j.catena.2017.08.005, 2017.

641   Chanda, A., Akhand, A., Manna, S., Dutta, S., Das, I., Hazra, S., Rao, K. H. and

642   Dadhwal, V. K.: Measuring daytime CO_2 fluxes from the inter-tidal mangrove soils of

643   Indian Sundarbans, Environ. Earth Sci., 72(2), 417–427, doi:10.1007/s12665-013-2962-

644   2, 2014.

645   Chauhan, R., Datta, A., Ramanathan, A. and Adhya, T. K.: Factors influencing spatio-

646   temporal variation of methane and nitrous oxide emission from a tropical mangrove of

647   eastern coast of India, Atmos. Environ., 107, 95–106,

648   doi:10.1016/j.atmosenv.2015.02.006, 2015.

649   Chen, G. C., Tam, N. F. Y. and Ye, Y.: Spatial and seasonal variations of atmospheric

650   N_2O and CO_2 fluxes from a subtropical mangrove swamp and their relationships with

651   soil characteristics, Soil Biol. Biochem., 48, 175–181,

652   doi:10.1016/j.soilbio.2012.01.029, 2012.

653   Chen, G. C., Ulumuddin, Y. I., Pramudji, S., Chen, S. Y., Chen, B., Ye, Y., Ou, D. Y.,

654   Ma, Z. Y., Huang, H. and Wang, J. K.: Rich soil carbon and nitrogen but low

655   atmospheric greenhouse gas fluxes from North Sulawesi mangrove swamps in

656   Indonesia, Sci. Total Environ., 487(1), 91–96, doi:10.1016/j.scitotenv.2014.03.140,

657   2014.

658   Chen, G. C. C., Tam, N. F. Y. F. Y. and Ye, Y.: Summer fluxes of atmospheric
659   greenhouse gases N2O, CH4 and CO2 from mangrove soil in South China, Sci. Total
660   Environ., 408(13), 2761–2767, doi:10.1016/j.scitotenv.2010.03.007, 2010.

661   Chowdhury, T. R., Bramer, L., Hoyt, D. W., Kim, Y. M., Metz, T. O., McCue, L. A.,
662   Diefenderfer, H. L., Jansson, J. K. and Bailey, V.: Temporal dynamics of CO2 and CH4
663   loss potentials in response to rapid hydrological shifts in tidal freshwater wetland soils,
664   Ecol. Eng., 114, 104–114, doi:10.1016/j.ecoleng.2017.06.041, 2018.

665   Chuang, P. C., Young, M. B., Dale, A. W., Miller, L. G., Herrera-Silveira, J. A. and
666   Paytan, A.: Methane and sulfate dynamics in sediments from mangrove-dominated
667   tropical coastal lagoons, Yucatan, Mexico, Biogeosciences, 13(10), 2981–3001, 2016.

668   Connell, W. E. and Patrick, W. H.: Sulfate Reduction in Soil: Effects of Redox Potential
669   and p H, Science (80-.)., 159(3810), 86–87, doi:10.1126/science.159.3810.86, 1968.

670   Coyne, M.: Soil Microbiology: An Exploratory Approach, Delmar Publishers, New
671   York, NY, USA., 1999.

672   Craig, H., Antwis, R. E., Cordero, I., Ashworth, D., Robinson, C. H., Osborne, T. Z.,
673   Bardgett, R. D., Rowntree, J. K. and Simpson, L. T.: Nitrogen addition alters
674   composition, diversity, and functioning of microbial communities in mangrove soils:
675   An   incubation   experiment,   Soil   Biol.   Biochem.,   153,   108076,
676   doi:10.1016/j.soilbio.2020.108076, 2021.

677   Dai, Z., Trettin, C. C., Li, C., Li, H., Sun, G. and Amatya, D. M.: Effect of Assessment
678   Scale on Spatial and Temporal Variations in CH4, CO2, and N2O Fluxes in a Forested
679   Wetland, Water, Air, Soil Pollut., 223(1), 253–265, doi:10.1007/s11270-011-0855-0,
680   2012.

681   Davidson, E. A., Verchot, L. V., Cattanio, J. H., Ackerman, I. L. and Carvalho, J. E. M.:
682   Effects of soil water content on soil respiration in forests and cattle pastures of eastern
683   Amazonia, Biogeochemistry, 48(1), 53–69, doi:10.1023/a:1006204113917, 2000.

684   Donato, D. C., Kauffman, J. B., Murdiyarso, D., Kurnianto, S., Stidham, M. and
685   Kanninen, M.: Mangroves among the most carbon-rich forests in the tropics, Nat.
686   Geosci., 4(5), 293–297, doi:10.1038/ngeo1123, 2011.

687   Dutta, M. K., Chowdhury, C., Jana, T. K. and Mukhopadhyay, S. K.: Dynamics and

688 exchange fluxes of methane in the estuarine mangrove environment of the Sundarbans,
689 NE coast of India, Atmos. Environ., 77, 631–639, doi:10.1016/j.atmosenv.2013.05.050,
690 2013.

691 Ehrenfeld, J. G.: Microsite differences in surface substrate characteristics in
692 Chamaecyparis swamps of the New Jersey Pinelands, Wetlands, 15(2), 183–189,
693 doi:10.1007/BF03160672, 1995.

694 El-Robrini, M., Alves, M. A. M. S., Souza Filho, P. W. M., El-Robrini M. H. S., Silva
695 Júnior, O. G. and França, C. F.: Atlas de Erosão e Progradação da zona costeira do
696 Estado do Pará − Região Amazônica: Áreas oceânica e estuarina, in Atlas de Erosão e
697 Progradação da Zona Costeira Brasileira, edited by D. Muehe, pp. 1–34, São Paulo.,
698 2006.

699 EPA, E. P. A.: Inventory of U.S. Greenhouse Gas Emissions and Sinks: 1990–2015.,
700 2017.

701 Fernandes, W. A. A. and Pimentel, M. A. da S.: Dinâmica da paisagem no entorno da
702 RESEX marinha de São João da Ponta/PA: utilização de métricas e geoprocessamento,
703 Caminhos Geogr., 20(72), 326–344, doi:10.14393/RCG207247140, 2019.

704 Ferreira, A. S., Camargo, F. A. O. and Vidor, C.: Utilização de microondas na avaliação
705 da biomassa microbiana do solo, Rev. Bras. Ciência do Solo, 23(4), 991–996,
706 doi:10.1590/S0100-06831999000400026, 1999.

707 Ferreira, S. da S.: Entre marés e mangues: paisagens territorializadas por pescadores da
708 resex marinha de São João da Ponta/PA /, Universidade Federal do Pará., 2017.

709 França, C. F. de, Pimentel, M. A. D. S. and Neves, S. C. R.: Estrutura Paisagística De
710 São João Da Ponta, Nordeste Do Pará, Geogr. Ensino Pesqui., 20(1), 130–142,
711 doi:10.5902/2236499418331, 2016.

712 Frankignoulle, M.: Field measurements of air-sea CO2 exchange, Limnol. Oceanogr.,
713 33(3), 313–322, 1988.

714 Friesen, S. D., Dunn, C. and Freeman, C.: Decomposition as a regulator of carbon
715 accretion in mangroves: a review, Ecol. Eng., 114, 173–178,
716 doi:10.1016/j.ecoleng.2017.06.069, 2018.

717 Fromard, F., Puig, H., Cadamuro, L., Marty, G., Betoulle, J. L. and Mougin, E.:
718 Structure, above-ground biomass and dynamics of mangrove ecosystems: new data

719   from French Guiana, Oecologia, 115(1), 39–53, doi:10.1007/s004420050489, 1998.

720   Gao, G. F., Zhang, X. M., Li, P. F., Simon, M., Shen, Z. J., Chen, J., Gao, C. H. and

721   Zheng, H. L.: Examining Soil Carbon Gas (CO_2, CH_4) Emissions and the Effect on

722   Functional Microbial Abundances in the Zhangjiang Estuary Mangrove Reserve, J.

723   Coast. Res., 36(1), 54–62, doi:10.2112/JCOASTRES-D-18-00107.1, 2020.

724   Gardunho, D. C. L.: Estimativas de biomassa acima do solo da floresta de mangue na

725   península de Ajuruteua, Bragança – PA, Federal University of Pará, Belém, Brazil.,

726   2017.

727   Hamilton, S. E. and Friess, D. A.: Global carbon stocks and potential emissions due to

728   mangrove deforestation from 2000 to 2012, Nat. Clim. Chang., 8(3), 240–244,

729   doi:10.1038/s41558-018-0090-4, 2018.

730   He, Y., Guan, W., Xue, D., Liu, L., Peng, C., Liao, B., Hu, J., Zhu, Q., Yang, Y., Wang,

731   X., Zhou, G., Wu, Z. and Chen, H.: Comparison of methane emissions among invasive

732   and native mangrove species in Dongzhaigang, Hainan Island, Sci. Total Environ., 697,

733   133945, doi:10.1016/j.scitotenv.2019.133945, 2019.

734   Hegde, U., Chang, T.-C. and Yang, S.-S.: Methane and carbon dioxide emissions from

735   Shan-Chu-Ku landfill site in northern Taiwan., Chemosphere, 52(8), 1275–1285,

736   doi:10.1016/S0045-6535(03)00352-7, 2003.

737   Herz, R.: Manguezais do Brasil, Instituto Oceanografico da Usp/Cirm, São Paulo,

738   Brazil., 1991.

739   Howard, J., Hoyt, S., Isensee, K., Telszewski, M. and Pidgeon, E.: Coastal Blue

740   Carbon: Methods for Assessing Carbon Stocks and Emissions Factors in Mangroves,

741   Tidal Salt Marshes, and Seagrasses, edited by J. Howard, S. Hoyt, K. Isensee, M.

742   Telszewski, and E. Pidgeon, International Union for Conservation of Nature, Arlington,

743   Virginia, USA. [online] Available from: http://www.unesco.org/new/en/natural-

744   sciences/ioc-oceans/sections-and-programmes/ocean-sciences/ocean-carbon/coastal-

745   blue-carbon/ (Accessed 11 September 2019), 2014.

746   IPCC: Climate Change 2001: Third Assessment Report of the IPCC, Cambridge., 2001.

747   Islam, K. R. and Weil, R. R.: Microwave irradiation of soil for routine measurement of

748   microbial   biomass   carbon,   Biol.   Fertil.   Soils,   27(4),   408–416,

749   doi:10.1007/s003740050451, 1998.

750 Kalembasa, S. J. and Jenkinson, D. S.: A comparative study of titrimetric and
751 gavimetric methods for determination of organic carbon in soil, J. Sci. Food Agric., 24,
752 1085–1090, 1973.

753 Kauffman, B. J., Donato, D. and Adame, M. F.: Protocolo para la medición, monitoreo
754 y reporte de la estructura, biomasa y reservas de carbono de los manglares, Bogor,
755 Indonesia., 2013.

756 Kauffman, J. B., Bernardino, A. F., Ferreira, T. O., Giovannoni, L. R., De Gomes, L. E.
757 O., Romero, D. J., Jimenez, L. C. Z. and Ruiz, F.: Carbon stocks of mangroves and salt
758 marshes of the Amazon region, Brazil, Biol. Lett., 14(9), doi:10.1098/rsbl.2018.0208,
759 2018.

760 Kreuzwieser, J., Buchholz, J. and Rennenberg, H.: Emission of Methane and Nitrous
761 Oxide by Australian Mangrove Ecosystems, Plant Biol., 5(4), 423–431, doi:10.1055/s-
762 2003-42712, 2003.

763 Kristensen, E., Bouillon, S., Dittmar, T. and Marchand, C.: Organic carbon dynamics in
764 mangrove ecosystems: A review, Aquat. Bot., 89(2), 201–219,
765 doi:10.1016/J.AQUABOT.2007.12.005, 2008.

766 Kristjansson, J. K., Schönheit, P. and Thauer, R. K.: Different Ks values for hydrogen
767 of methanogenic bacteria and sulfate reducing bacteria: An explanation for the apparent
768 inhibition of methanogenesis by sulfate, Arch. Microbiol., 131(3), 278–282,
769 doi:10.1007/BF00405893, 1982.

770 Lekphet, S., Nitisoravut, S. and Adsavakulchai, S.: Estimating methane emissions from
771 mangrove area in Ranong Province, Thailand, Songklanakarin J. Sci. Technol. ·, 27(1),
772 153–163 [online] Available from: https://www.researchgate.net/publication/26473398
773 (Accessed 29 January 2019), 2005.

774 Maher, D. T., Call, M., Santos, I. R. and Sanders, C. J.: Beyond burial: Lateral
775 exchange is a significant atmospheric carbon sink in mangrove forests, Biol. Lett.,
776 14(7), 1–4, doi:10.1098/rsbl.2018.0200, 2018.

777 Mahesh, P., Sreenivas, G., Rao, P. V. N. N., Dadhwal, V. K., Sai Krishna, S. V. S. S.
778 and Mallikarjun, K.: High-precision surface-level CO2 and CH4 using off-axis
779 integrated cavity output spectroscopy (OA-ICOS) over Shadnagar, India, Int. J. Remote
780 Sens., 36(22), 5754–5765, doi:10.1080/01431161.2015.1104744, 2015.

781 Marchand, C.: Soil carbon stocks and burial rates along a mangrove forest
782 chronosequence (French Guiana), For. Ecol. Manage., 384, 92–99,
783 doi:10.1016/j.foreco.2016.10.030, 2017.

784 McEwing, K. R., Fisher, J. P. and Zona, D.: Environmental and vegetation controls on
785 the spatial variability of CH4 emission from wet-sedge and tussock tundra ecosystems
786 in the Arctic, Plant Soil, 388(1–2), 37–52, doi:10.1007/s11104-014-2377-1, 2015.

787 Megonigal, J. P. and Schlesinger, W. H.: Methane-limited methanotrophy in tidal
788 freshwater swamps, Global Biogeochem. Cycles, 16(4), 35-1-35–10,
789 doi:10.1029/2001GB001594, 2002.

790 Menezes, M. P. M. de, Berger, U. and Mehlig, U.: Mangrove vegetation in Amazonia :
791 a review of studies from the coast of Pará and Maranhão States , north Brazil, Acta
792 Amaz., 38(3), 403–420, doi:10.1590/S0044-59672008000300004, 2008.

793 Milucka, J., Kirf, M., Lu, L., Krupke, A., Lam, P., Littmann, S., Kuypers, M. M. M. and
794 Schubert, C. J.: Methane oxidation coupled to oxygenic photosynthesis in anoxic
795 waters, ISME J., 9(9), 1991–2002, doi:10.1038/ismej.2015.12, 2015.

796 Monz, C. A., Reuss, D. E. and Elliott, E. T.: Soil microbial biomass carbon and nitrogen
797 estimates using 2450 MHz microwave irradiation or chloroform fumigation followed by
798 direct extraction, Agric. Ecosyst. Environ., 34(1–4), 55–63, doi:10.1016/0167-
799 8809(91)90093-D, 1991.

800 Neubauer, S. C. and Megonigal, J. P.: Moving Beyond Global Warming Potentials to
801 Quantify the Climatic Role of Ecosystems, Ecosystems, 18(6), 1000–1013,
802 doi:10.1007/S10021-015-9879-4/TABLES/2, 2015.

803 Nóbrega, G. N., Ferreira, T. O., Siqueira Neto, M., Queiroz, H. M., Artur, A. G.,
804 Mendonça, E. D. S., Silva, E. D. O. and Otero, X. L.: Edaphic factors controlling
805 summer (rainy season) greenhouse gas emissions (CO2 and CH4) from semiarid
806 mangrove soils (NE-Brazil), Sci. Total Environ., 542, 685–693,
807 doi:10.1016/j.scitotenv.2015.10.108, 2016.

808 Norman, J. M., Kucharik, C. J., Gower, S. T., Baldocchi, D. D., Crill, P. M., Rayment,
809 M., Savage, K. and Striegl, R. G.: A comparison of six methods for measuring soil-
810 surface carbon dioxide fluxes, J. Geophys. Res. Atmos., 102(D24), 28771–28777,
811 doi:10.1029/97JD01440, 1997.

812   Peel, M. C., Finlayson, B. L. and McMahon, T. A.: Updated world map of the Köppen-
813   Geiger climate classification, Hydrol. Earth Syst. Sci., 11(5), 1633–1644,
814   doi:10.1002/ppp.421, 2007.

815   Poffenbarger, H. J., Needelman, B. A. and Megonigal, J. P.: Salinity Influence on
816   Methane Emissions from Tidal Marshes, Wetlands, 31(5), 831–842,
817   doi:10.1007/s13157-011-0197-0, 2011.

818   Prost, M. T., Mendes, A. C., Faure, J. F., Berredo, J. F., Sales, M. E. ., Furtado, L. G.,
819   Santana, M. G., Silva, C. A., Nascimento, I. ., Gorayeb, I., Secco, M. F. and Luz, L.:
820   Manguezais e estuários da costa paraense: exemplo de estudo multidisciplinar integrado
821   (Marapanim e São Caetano de Odivelas), in Ecossistemas costeiros: impactos e gestão
822   ambiental, edited by M. T. Prost and A. Mendes, pp. 25–52, FUNTEC and Museu
823   Paraense Emílio Goeldi, Belém, Brazil., 2001.

824   Purvaja, R. and Ramesh, R.: Natural and Anthropogenic Methane Emission from
825   Coastal Wetlands of South India, Environ. Manage., 27(4), 547–557,
826   doi:10.1007/s002670010169, 2001.

827   Purvaja, R., Ramesh, R. and Frenzel, P.: Plant-mediated methane emission from an
828   Indian mangrove, Glob. Chang. Biol., 10(11), 1825–1834, doi:10.1111/j.1365-
829   2486.2004.00834.x, 2004.

830   Reeburgh, W. S.: Oceanic Methane Biogeochemistry, Chem. Rev., 2, 486–513,
831   doi:10.1021/cr050362v, 2007.

832   Robertson, A. I., Alongi, D. M. and Boto, K. G.: Food chains and carbon fluxes, in
833   Coastal and Estuarine Studies, edited by A. I. Robertson and D. M. Alongi, pp. 293–
834   326, American Geophysical Union., 1992.

835   Rocha, A. S.: Caracterização física do estuário do rio Mojuim em São Caetano de
836   Odivelas - Pa, Universidade Federal do Pará., 2015.

837   Rollnic, M., Costa, M. S., Medeiros, P. R. L. and Monteiro, S. M.: Tide Influence on
838   Suspended Matter Transport in an Amazonian Estuary, in Journal of Coastal Research,
839   vol. 85, pp. 121–125, Allen Press., 2018.

840   Rosentreter, J. A., Maher, D. T., Erler, D. V., Murray, R. H. and Eyre, B. D.: Methane
841   emissions partially offset "blue carbon" burial in mangroves, Sci. Adv., 4(6), eaao4985,
842   doi:10.1126/sciadv.aao4985, 2018a.

843   Rosentreter, J. A., Maher, D. . T., Erler, D. V. V., Murray, R. and Eyre, B. D. D.:

844   Seasonal and temporal CO2 dynamics in three tropical mangrove creeks – A revision of

845   global mangrove CO2 emissions, Geochim. Cosmochim. Acta, 222, 729–745,

846   doi:10.1016/j.gca.2017.11.026, 2018b.

847   Roslev, P. and King, G. M.: Regulation of methane oxidation in a freshwater wetland by

848   water table changes and anoxia, FEMS Microbiol. Ecol., 19(2), 105–115,

849   doi:10.1111/j.1574-6941.1996.tb00203.x, 1996.

850   Sahu, S. K. and Kathiresan, K.: The age and species composition of mangrove forest

851   directly influence the net primary productivity and carbon sequestration potential,

852   Biocatal. Agric. Biotechnol., 20, 101235, doi:10.1016/j.bcab.2019.101235, 2019.

853   Salum, R. B., Souza-Filho, P. W. M., Simard, M., Silva, C. A., Fernandes, M. E. B.,

854   Cougo, M. F., do Nascimento, W. and Rogers, K.: Improving mangrove above-ground

855   biomass estimates using LiDAR, Estuar. Coast. Shelf Sci., 236, 106585,

856   doi:10.1016/j.ecss.2020.106585, 2020.

857   Schmidt, M. W. I., Torn, M. S., Abiven, S., Dittmar, T., Guggenberger, G., Janssens, I.

858   A., Kleber, M., Kögel-Knabner, I., Lehmann, J., Manning, D. A. C., Nannipieri, P.,

859   Rasse, D. P., Weiner, S. and Trumbore, S. E.: Persistence of soil organic matter as an

860   ecosystem property, Nature, 478(7367), 49–56, doi:10.1038/nature10386, 2011.

861   Segarra, K. E. A., Schubotz, F., Samarkin, V., Yoshinaga, M. Y., Hinrichs, K. U. and

862   Joye, S. B.: High rates of anaerobic methane oxidation in freshwater wetlands reduce

863   potential atmospheric methane emissions, Nat. Commun., 6(1), 1–8,

864   doi:10.1038/ncomms8477, 2015.

865   Shiau, Y.-J. and Chiu, C.-Y.: Biogeochemical Processes of C and N in the Soil of

866   Mangrove Forest Ecosystems, Forests, 11(5), 492, doi:10.3390/f11050492, 2020.

867   Shiau, Y. J., Cai, Y., Lin, Y. Te, Jia, Z. and Chiu, C. Y.: Community Structure of Active

868   Aerobic Methanotrophs in Red Mangrove (Kandelia obovata) Soils Under Different

869   Frequency of Tides, Microb. Ecol., 75(3), 761–770, doi:10.1007/s00248-017-1080-1,

870   2018.

871   Sihi, D., Davidson, E. A., Chen, M., Savage, K. E., Richardson, A. D., Keenan, T. F.

872   and Hollinger, D. Y.: Merging a mechanistic enzymatic model of soil heterotrophic

873   respiration into an ecosystem model in two AmeriFlux sites of northeastern USA,

874 Agric. For. Meteorol., 252, 155–166, doi:10.1016/J.AGRFORMET.2018.01.026, 2018.

875 Souza Filho, P. W. M.: Costa de manguezais de macromaré da Amazônia: cenários
876 morfológicos, mapeamento e quantificação de áreas usando dados de sensores remotos,
877 Rev. Bras. Geofísica, 23(4), 427–435, doi:10.1590/S0102-261X2005000400006, 2005.

878 Sparling, G. P. and West, A. W.: A direct extraction method to estimate soil microbial
879 C: calibration in situ using microbial respiration and 14C labelled cells, Soil Biol.
880 Biochem., 20(3), 337–343, doi:10.1016/0038-0717(88)90014-4, 1988.

881 Sundqvist, E., Vestin, P., Crill, P., Persson, T. and Lindroth, A.: Short-term effects of
882 thinning, clear-cutting and stump harvesting on methane exchange in a boreal forest,
883 Biogeosciences, 11(21), 6095–6105, doi:10.5194/bg-11-6095-2014, 2014.

884 Valentim, M., Monteiro, S. and Rollnic, M.: The Influence of Seasonality on Haline
885 Zones in An Amazonian Estuary, J. Coast. Res., 85, 76–80, doi:10.2112/SI85-016.1,
886 2018.

887 Valentine, D. L.: Emerging Topics in Marine Methane Biogeochemistry, Ann. Rev.
888 Mar. Sci., 3(1), 147–171, doi:10.1146/annurev-marine-120709-142734, 2011.

889 Vance, E. D., Brookes, P. C. and Jenkinson, D. S.: An extraction method for measuring
890 soil microbial biomass C, Soil Biol. Biochem., 19(6), 703–707, doi:10.1016/0038-
891 0717(87)90052-6, 1987.

892 Verchot, L. V., Davidson, E. A., Cattânio, J. H. and Ackerman, I. L.: Land-use change
893 and biogeochemical controls of methane fluxes in soils of eastern Amazonia,
894 Ecosystems, 3(1), 41–56, doi:10.1007/s100210000009, 2000.

895 Whalen, S. C.: Biogeochemistry of Methane Exchange between Natural Wetlands and
896 the Atmosphere, Environ. Eng. Sci., 22(1), 73–94, doi:10.1089/ees.2005.22.73, 2005.

897 Xu, X., Elias, D. A., Graham, D. E., Phelps, T. J., Carroll, S. L., Wullschleger, S. D. and
898 Thornton, P. E.: A microbial functional group-based module for simulating methane
899 production and consumption: Application to an incubated permafrost soil, J. Geophys.
900 Res. Biogeosciences, 120(7), 1315–1333, doi:10.1002/2015JG002935, 2015.

901 Yang, S. S. and Chang, H. L.: Effect of environmental conditions on methane
902 production and emission from paddy soil, Agric. Ecosyst. Environ., 69(1), 69–80,
903 doi:10.1016/S0167-8809(98)00098-X, 1998.

904